

# Depletion potentials near geometrically structured substrates

P. BRYK<sup>1,2</sup>, R. ROTH<sup>1,2</sup>, M. SCHOEN<sup>3</sup> and S. DIETRICH<sup>1,2</sup>

<sup>1</sup> *Max-Planck-Institut für Metallforschung – Heisenbergstr. 3, D-70569 Stuttgart, Germany*

<sup>2</sup> *Institut für Theoretische und Angewandte Physik, Universität Stuttgart – Pfaffenwaldring 57, D-70569 Stuttgart, Germany*

<sup>3</sup> *Stranski-Laboratorium für Physikalische und Theoretische Chemie, Sekretariat TC7, Technische Universität Berlin – Strasse des 17.Juni 124, D-10623 Berlin, Germany*

PACS. 61.20.Gy – Theory and models of liquid structure.

PACS. 82.70.Dd – Colloids.

**Abstract.** – Using the recently developed so-called White Bear version of Rosenfeld’s Fundamental Measure Theory we calculate the depletion potentials between a hard-sphere colloidal particle in a solvent of small hard spheres and simple models of geometrically structured substrates: a right-angled wedge or edge. In the wedge geometry, there is a strong attraction beyond the corresponding one near a planar wall that significantly influences the structure of colloidal suspensions in wedges. In accordance with an experimental study, for the edge geometry we find a free energy barrier of the order of several  $k_B T$  which repels a big colloidal particle from the edge.

When a colloidal suspension contains particles of different size, depletion forces arise between big particles due to excluded volume effects. If a colloidal suspension is prepared such that electrostatic interactions are screened and only hard-core repulsive interactions are left, these forces are attractive at small distances [1] and can exhibit a potential barrier and an oscillatory tail for large separations [2, 3, 4, 5]. The same forces also arise if a big colloidal particle  $b$  (diameter  $\sigma_b$ ) suspended in a solvent of small particles  $s$  (diameter  $\sigma_s$ ) approaches a wall. The depletion forces for hard-sphere models of bulk colloidal suspensions, as well as colloidal suspensions close to structureless walls have been the subject of many theoretical studies. Technical developments during the last decade made it possible to prepare well-defined, monodisperse colloidal suspensions and with the help of video-microscopy [6] and total internal reflection microscopy [7, 8, 9] such depletion potentials can be now measured directly and compared quantitatively with theoretical predictions.

On the other hand, the behavior of colloidal suspensions close to *structured* walls and resulting depletion potentials have not yet been investigated in depth. Such situations arise naturally for example close to a corner in a container for colloidal suspensions. Geometrically structured substrates with a dedicated design have been used to control the growth of colloidal crystals [10]. In this context Dinsmore et al. [11] studied the motion of colloidal ”hard-spheres“

near the edge of a terrace by means of video-microscopy. In the direction perpendicular to the edge they found a free-energy barrier approximately two times the mean thermal energy. Dinsmore et al. suggested that localized entropic force-fields created by various structures of the substrate can be used to control the movement of colloidal particles and, consequently, could be used to create highly ordered arrays of colloidal particles.

Recently, Kinoshita et al. [12,13] have studied depletion potentials of hard spheres close to the substrate exhibiting various geometrical features by means of first-order Ornstein-Zernike (FOOZ) integral equations. Using correlation functions of the bulk hard-sphere fluid as input, they calculated the potential of mean force between a big particle and an edge or hemispherical hole in a planar substrate (mimicking key and lock steric interactions between macromolecules). However, FOOZ theory assumes that the correlation functions close to the surface are the same as in the bulk, which gives rise to discrepancies in predicting packing effects as compared to simulation data. For geometrically structured surfaces, where these packing effects may be very pronounced like, e.g. in a wedge, the FOOZ approach is expected to be even less reliable.

Depletion forces in the bulk or close to planar walls have been studied also by means of molecular dynamics [2] and Monte Carlo (MC) simulations [3]. While being computationally quite demanding, these studies serve as a useful test for various theories. However, the study of the fluid structure near geometrically structured substrates is computationally even more costly than for planar walls so that there are only few such studies [14,15,16].

A versatile approach to study depletion potentials close to arbitrarily shaped substrates has been proposed in Refs. [4] and [5]. According to this theory the depletion potential is evaluated using the potential distribution theorem [4,5,17,18] on the basis of the density profile of the small spheres close to the substrate without the big sphere. This method is valid for all geometries of the substrate, but explicit calculations so far have been carried out only for structureless planar walls [4] or spherically curved substrates [19].

Here we apply the aforementioned scheme to calculate the depletion potential of a single big hard sphere close to a right-angled wedge or edge. Within this approach it is important to determine accurately the density profile  $\rho_s(\mathbf{r})$  of the small spheres close to the edge or wedge where it varies most rapidly.

The calculation of the density profile of a hard-sphere fluid close to planar or spherical structureless walls constitutes a standard problem in the statistical mechanics of fluids which lends itself to be solved by density functional theory (DFT). It has emerged that Rosenfeld's Fundamental Measure Theory (FMT) [20] is one of the most accurate DFTs if compared with simulations for either one-component, binary [21] or polydisperse [22] hard-sphere fluids close to a hard-wall. However, for complex geometries like wedges or edges there are only a few comparisons of DFT and simulations available [23,24]. Thus before calculating the depletion potentials we test the accuracy of the DFT against MC simulations.

The key approximation in every density functional theory resides in an expression for the excess (over the ideal gas) intrinsic free energy  $\mathcal{F}_{ex}^{(hs)}[\rho_i(\mathbf{r})]$  of an inhomogeneous fluid as a functional of local densities  $\rho_i(\mathbf{r})$ . Within the framework of FMT [20] one has

$$\beta\mathcal{F}_{ex}^{(hs)}[\{\rho_i\}] = \int d^3r \Phi(\{n_\alpha\}), \quad (1)$$

where  $\beta = (k_B T)^{-1}$ ,  $k_B$  is the Boltzmann constant, and  $T$  is the temperature. The excess free energy density  $\Phi$  is a function of weighted densities

$$n_\alpha(\mathbf{r}) = \sum_{i=s,b} \int d^3r' \rho_i(\mathbf{r}') w_i^{(\alpha)}(\mathbf{r} - \mathbf{r}'), \quad (2)$$

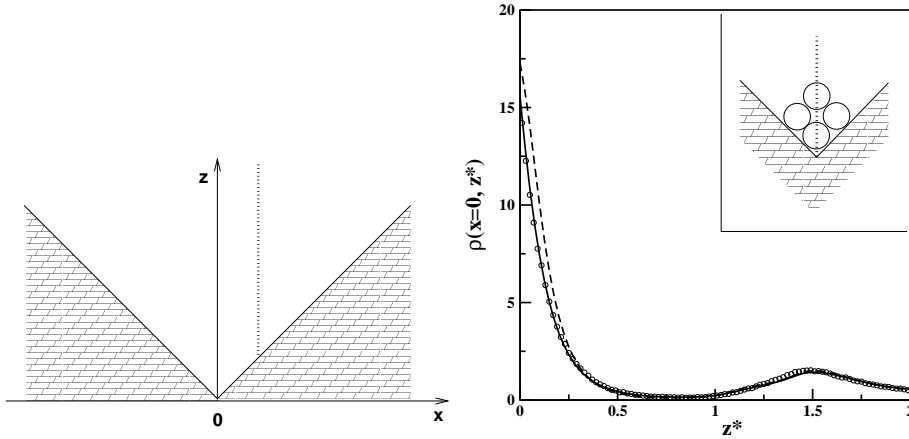


Fig. 1 – Schematic representation of a right-angled wedge  $z_w(x) = |x|$ . The dotted line indicates a possible cut along which the density profiles are presented.

Fig. 2 – Density profile  $\rho(x=0, z^*)$  from MC (circles), *RF* version (dashed line) and *WB* version of FMT (solid line) for a bulk density  $\rho_s = 0.7$ , with  $z^* = \frac{(z-z_w)}{\sigma_s} - \frac{1}{\sqrt{2}}$ . The inset illustrates this density distribution by showing the corresponding typical particle configuration. Here and below lengths and number densities are given in units of  $\sigma_s$  and  $\sigma_s^{-3}$ , respectively.

with six different geometrical weight functions  $w_i^{(\alpha)}$  per component  $i$  (four scalar and two vector-like). In the present problem all quantities are translationally invariant along the wedge or edge which we choose as the  $y$ -direction. In order to calculate weighted densities  $n_\alpha(x, z)$  in an efficient way we have applied the two-dimensional Fast Fourier Transform.

From a variety of expressions for  $\Phi$  here we select two of them. The first one is the original Rosenfeld functional (*RF*) [20]

$$\Phi^{(RF)}(\{n_\alpha\}) = -n_0 \ln(1 - n_3) + \frac{n_1 n_2 - \mathbf{n}_1 \cdot \mathbf{n}_2}{1 - n_3} + \frac{n_2^3 - 3n_2 \mathbf{n}_2 \cdot \mathbf{n}_2}{24\pi(1 - n_3)^2}, \quad (3)$$

based on the Percus-Yevick compressibility equation of state. As pointed out in Ref. [25] this approximation does not render a freezing transition. Our second choice is based on the Boublik-Mansoori-Carnahan-Starling-Leland equation of state [26, 27] as proposed by Tarazona [28] and Roth *et al.* [29] (see also Ref. [30] where the same functional has been proposed, too). Moreover this choice implements a modification proposed in Ref. [25] (the so-called antisymmetrized form,  $Q = 3$ ) that allows for the occurrence of a freezing transition:

$$\Phi^{(WB)}(\{n_\alpha\}) = -n_0 \ln(1 - n_3) + \frac{n_1 n_2 - \mathbf{n}_1 \cdot \mathbf{n}_2}{1 - n_3} + n_2^3 (1 - \xi^2)^3 \frac{n_3 + (1 - n_3)^2 \ln(1 - n_3)}{36\pi n_3^2 (1 - n_3)^2}, \quad (4)$$

where  $\xi(\mathbf{r}) = |\mathbf{n}_2(\mathbf{r})|/n_2(\mathbf{r})$ . Following the nomenclature in Ref. [29] this DFT version is denoted *WB* (“White Bear”). The density profiles are obtained by solving the Euler-Lagrange equations corresponding to the minimum of the grand potential functional.

The Monte Carlo simulations have been performed in a grand canonical ensemble according to a procedure described in detail in Ref. [16]. However, we emphasize that unlike in Ref. [16] the MC-generated density profiles presented below have not been smoothed but are instead the “raw” data generated in MC simulations with no further post-simulation processing applied.

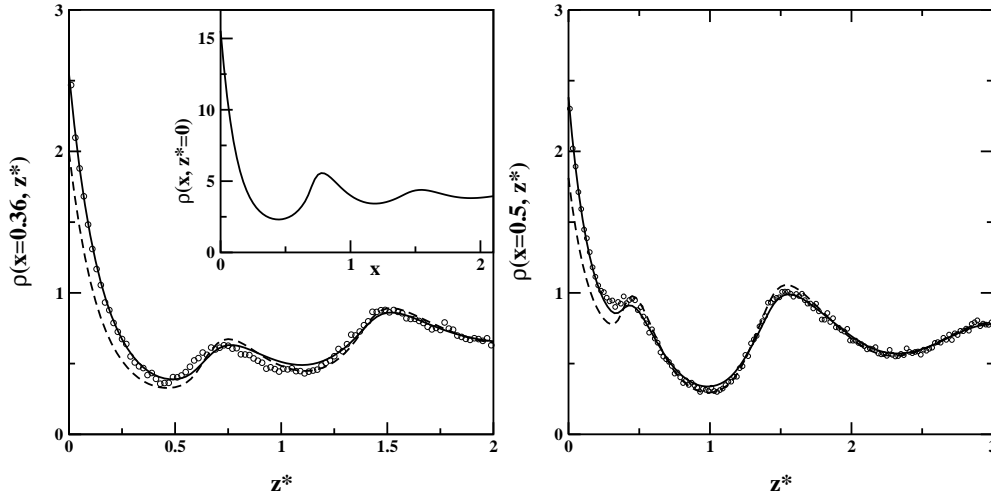


Fig. 3 – The density profile  $\rho(x = 0.36, z^*)$  from MC simulations (circles), *RF* version (dashed line), and *WB* version (solid lines) evaluated for the bulk density  $\rho_s = 0.7$ . The inset shows the contact value of the density profile resulting from the White Bear version as function of  $x$ .

Fig. 4 – The density profile  $\rho(x = 0.5, z^*)$  from MC simulations (circles), *RF* version (dashed line), and *WB* version (solid line) evaluated for the bulk density  $\rho_s = 0.7$ .

The comparison of the DFT and MC density profiles has been carried out only for the wedge geometry, because in this geometry packing effects are much more pronounced than for the edge and thus presents the more severe challenge for DFT. The dependence of the density profile  $\rho_s = \rho_s(x, z)$  on two spatial variables is illustrated by vertical cuts along the lines  $x = \text{const}$  (see fig. 1). In the following all length scales are expressed in units of  $\sigma_s$ , the diameter of the small spheres, and the number densities in units of  $\sigma_s^{-3}$ .

Figures 2-4 show such MC density profiles (circles) and the corresponding ones from DFT (dashed and solid lines). The comparison with the MC data shows that the *WB* version represents a noticeable improvement over the *RF* version in particular for  $z^* = \frac{z - z_w}{\sigma_s} - \frac{1}{\sqrt{2}} < 0.5$ . Along the line  $x = 0$  (see fig. 2) the contact value of the profile resulting from the *WB* version is 15.54 while from *RF* 17.29, i.e., a difference of ca. 10%. Also for  $x = 0.36$  (see fig. 3) the *WB* version agrees better with the MC data than *RF* again in particular for  $z^* < 0.5$ . The contact value  $\rho_s^{(WB)}(x = 0.36, z^* = 0) = 2.55$  differs from  $\rho_s^{(RF)}(x = 0.36, z^* = 0) = 1.99$  by ca. 20%.

The large variations (between 15.5 and 2.5) of the contact densities for  $0 \leq x \leq 0.5$  (see the inset in fig. 3) illustrate the strong packing effects in this system. In fig. 4 for  $x = 0.5$  a small plateau develops around  $z^* = 0.5$ . The *RF* version exaggerates this feature considerably and leads to a contact value  $\rho_s^{(RF)}(x = 0.5, z^* = 0) = 1.81$  whereas the *WB* version reproduces the plateau more accurately leading to a contact value  $\rho_s^{(WB)}(x = 0.5, z^* = 0) = 2.38$ .

We refrain from comparing directly contact values from DFT with those from MC because in the MC simulations  $\rho(x, z)$  has to be calculated as a histogram on a two-dimensional grid. Even though the mesh width  $\delta x = \delta z = 0.02$  of this grid is small, an extrapolation scheme is required to obtain an estimate for the contact value. This extrapolation scheme is particularly delicate near the core of the wedge where  $\rho(x, z)$  varies rapidly. However, inspection of figs. 2-

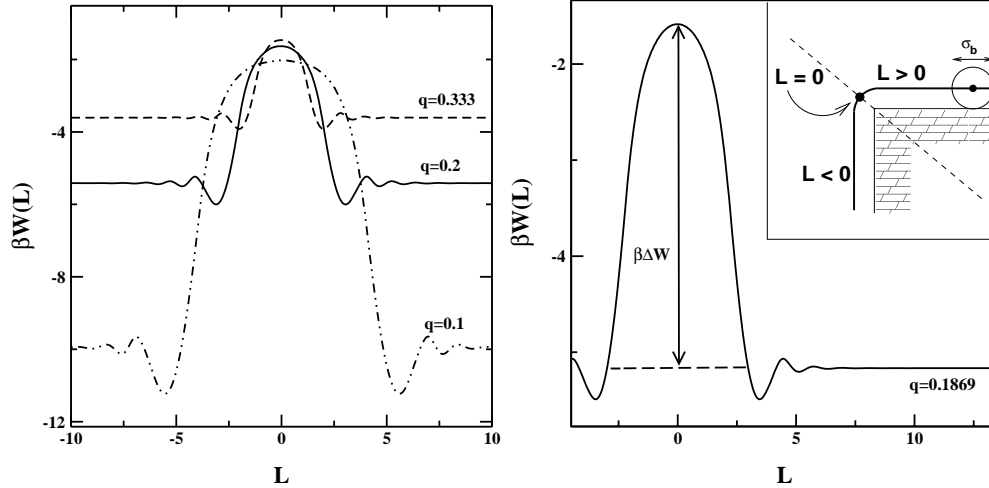


Fig. 5 – The depletion potential of the big colloidal particle close to the edge along the line of closest contact (see the inset in fig.(6)). The packing fraction of the small spheres is  $\eta = 0.366$ . The dashed, solid, and dashed-dotted lines correspond to the size ratios  $q \equiv \sigma_s/\sigma_b = 0.333, 0.2,$  and  $0.1,$  respectively.

Fig. 6 – The depletion potential along the line of closest contact between the big colloidal particle and the  $90^\circ$  right-angled edge (inset) evaluated for  $\sigma_b = 5.35\sigma_s$  and  $\eta = 0.3$

4 leads to the expectation that the *WB* version of DFT reproduces the actual contact values rather accurately. We have carried out calculations also for lower bulk densities finding a similar (or even better) agreement between DFT and simulations. Thus we conclude that FMT predicts accurately the structure of the hard-sphere fluid in a hard wedge; its *WB* version improves the agreement with simulations near the core of the wedge, where packing effects are particularly pronounced.

Reassured by the quality of the density profiles resulting from DFT, we have calculated the depletion potentials  $W$  near a hard wedge and edge based on the *WB* version of DFT. We use the fact that in the limit of a dilute solution of big particles  $\beta W$  can be calculated from the density distribution of the small spheres unperturbed by the presence of the big one. It has been shown [4, 5] that in the dilute limit of the big spheres the depletion potential of species  $b$  at a point  $\mathbf{r}$  can be expressed in terms of the difference between the one-particle direct correlation function  $c_b^{(1)}$  in the bulk ( $\mathbf{r} \rightarrow \infty$ ) and at  $\mathbf{r}$ :

$$\beta W(\mathbf{r}) = \lim_{\rho_b \rightarrow 0} \left( c_b^{(1)}(\mathbf{r} \rightarrow \infty) - c_b^{(1)}(\mathbf{r}) \right) \quad (5)$$

with  $c_b^{(1)}(\mathbf{r}) = -\delta\mathcal{F}_{ex}/\delta\rho_b(\mathbf{r})$  within DFT [31].

In fig. 5 we show  $\beta W$  for size ratios  $q^{-1} \equiv \sigma_b/\sigma_s = 3, 5,$  and  $10$  at a hard edge for a bulk packing fraction of the small spheres  $\eta = \frac{\pi}{6}\rho_s\sigma_s^3 = 0.366$ . The depletion potential is evaluated along the line of contact between the big sphere and the edge (see the inset in fig. 6);  $L$  parametrizes a path on this line. For  $L \rightarrow \pm\infty$  the depletion potential between a planar hard wall and a big sphere is recovered. Upon approaching the edge, oscillations in the contact value of  $\beta W$  occur. At the corner there is a pronounced maximum in the (still attractive)

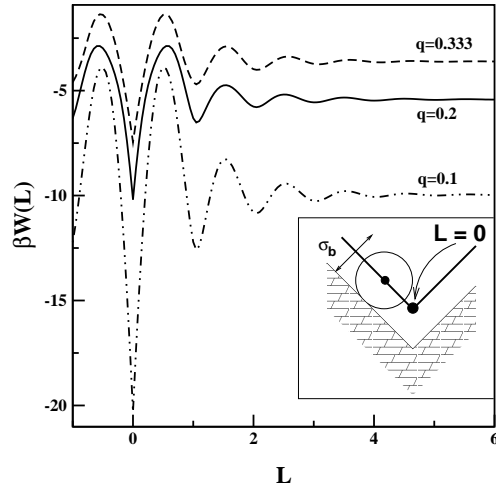


Fig. 7 – The depletion potential of the big colloidal particle close to the wedge taken along the line of closest contact. The packing fraction of the small spheres is  $\eta = 0.366$ . The dashed, solid and dotted-dashed lines correspond to the size ratios  $q = 0.333, 0.5$  and  $0.1$ , respectively.

depletion potential. The value of  $\beta W$  at the maximum, i.e., at  $L = 0$  equals  $-1.5, -1.6$  and  $-2.0$  for  $q = 0.333, 0.2$ , and  $0.1$ , respectively. This maximum represents an effective repulsive barrier repelling a big colloidal particle approaching the edge from the side and practically preventing it from passing around the corner. The difference  $\beta\Delta W$  between the depletion potential at the planar hard wall and at the corner is a quantitative measure of the barrier height. The barrier height increases upon decreasing  $q$  and for the system shown in fig 5 it equals  $2.1, 3.8$ , and  $8.0$ , respectively.

In fig. 6 we present  $\beta W$  along the line of contact for a system mimicking the experimental system studied by Dinsmore et al. [11]. Theoretically we find  $\beta\Delta W \simeq 3.6$  which is larger than the corresponding result obtained from the Asakura-Oosawa approximation ( $\beta\Delta W \simeq 3$ , [11]) which treats the solvent as an ideal gas. The experimental value quoted for the barrier height ( $\simeq 2$ ) [11] is smaller than both theoretical results. This is expected because for the theoretical value the big particle is assumed to move along the line of contact with the wall whereas experimentally on average some of the big particles monitored experimentally happen to be located slightly above the surface.  $\beta\Delta W$  reaches a value of 2 at a normal distance of about  $0.2\sigma_s$ . The depletion potentials shown in figs. 5 and 6 exhibit an oscillatory behavior due to correlation effects missed by the Asakura-Oosawa approximation which holds only in the limit  $\eta \rightarrow 0$ . These correlations lead to a minimum of  $\beta W$  at  $L \simeq 3.5$  next to the main peak (see fig. 6), which is the global minimum and is also visible in the experimental depletion potential [11].

In fig. 7 we show  $\beta W$  along the line of contact for a single big hard sphere in a right-angled hard wedge for  $\eta = 0.366$  and  $q = 0.333, 0.2$ , and  $0.1$ . As in fig. 5 we focus on the depletion potential along the line of contact between the big sphere and the wedge surface (see the inset in fig. 7). Again in the limit  $L \rightarrow \pm\infty$  the contact value of  $\beta W$  between a planar hard wall and a big hard sphere is recovered. Near the core of the wedge oscillations occur which are more pronounced than for the corresponding edge cases. Attraction is strongest directly in the corner where  $\beta W = -7.5, -10.2$ , and  $-20.3$  for  $q = 0.333, 0.2$ , and  $0.1$ , respectively. This is roughly twice the corresponding contact values at a planar hard wall ( $-3.6, -5.4$ , and  $-10.0$ ).

This potential is expected to promote highly ordered structures of big colloids in the core of the wedge. The pronounced oscillations of the depletion potential upon approaching the core of the wedge along the walls can lead to additional ordering.

We have studied depletion potentials near geometrically structured substrates. It has turned out that the recently developed “White Bear” version [29] of Fundamental Measure Theory in its antisymmetrized form [25] is able to reproduce accurately the structure of the hard-sphere fluid in a hard wedge as obtained from Monte Carlo simulations. The free energy barrier repelling a big colloidal particle from a substrate edge can be of the order of several  $k_B T$  in accordance with experiments [11]. In conclusion, the results presented in this letter demonstrate that geometrically structured substrates create strong and oscillatory entropic force fields that may significantly affect the structure and hence the properties of colloidal suspensions near their container walls.

## REFERENCES

- [1] ASAKURA S. and OOSAWA F., *J. Chem. Phys.*, **22** (1954) 1255.
- [2] DICKMAN R., ATTARD P. and SIMONIAN V., *J. Chem. Phys.*, **107** (1997) 205.
- [3] BIBEN T., BLADON P. and FRENKEL D., *J. Phys. Condens. Matter*, **8** (1996) 10799.
- [4] ROTH R., EVANS R. and DIETRICH S., *Phys. Rev. E*, **62** (2000) 5360.
- [5] GÖTZELMANN B., ROTH R., DIETRICH S., DIJKSTRA M. and EVANS R., *Europhys. Lett.*, **47** (1999) 398.
- [6] CROCKER J. C., MATTEO J. A., DINSMORE A. D. and YODH A. G., *Phys. Rev. Lett.*, **82** (1999) 4352.
- [7] RUDHARDT D., BECHINGER C. and LEIDERER P., *Phys. Rev. Lett.*, **81** (1998) 1330.
- [8] BECHINGER C., RUDHARDT D., LEIDERER P., ROTH R. and DIETRICH S., *Phys. Rev. Lett.*, **83** (1999) 3960.
- [9] HELDEN L., ROTH R., KOENDERINK G. H., LEIDERER P. and BECHINGER C., *Phys. Rev. Lett.*, **90** (48301) 2003.
- [10] YIN Y. and XIA Y., *Adv. Mater.*, **14** (2002) 605.
- [11] DINSMORE A. D., YODH A. G. and PINE D. J., *Nature*, **383** (1996) 239.
- [12] KINOSHITA M. and OGUNI T., *Chem. Phys. Lett.*, **351** (2002) 79.
- [13] KINOSHITA M., *J. Chem. Phys.*, **116** (2002) 3493.
- [14] DIESTLER D. J. and SCHOEN M., *Phys. Rev. E*, **62** (2000) 6615.
- [15] SCHOEN M., *Colloids and Surf. A: Physicochem. Eng. Asp.*, **206** (2002) 253.
- [16] SCHOEN M. and DIETRICH S., *Phys. Rev. E*, **56** (1997) 499.
- [17] HENDERSON J. R., *Mol. Phys.*, **50** (1983) 741.
- [18] WIDOM B., *J. Chem. Phys.*, **39** (1963) 2808.
- [19] ROTH R., GÖTZELMANN B. and DIETRICH S., *Phys. Rev. Lett.*, **83** (1999) 448.
- [20] ROSENFELD Y., *Phys. Rev. Lett.*, **63** (1989) 980.
- [21] ROTH R. and DIETRICH S., *Phys. Rev. E*, **62** (2000) 6926.
- [22] PIZIO O., PATRYKIEJEV A. and SOKOŁOWSKI S., *Mol. Phys.*, **99** (2001) 57.
- [23] HENDERSON D., SOKOŁOWSKI S. and WASAN D. T., *Phys. Rev. E*, **57** (1998) 5539.
- [24] JAGANNATHAN K. and YETHIRAJ A., *J. Chem. Phys.*, **116** (2002) 5795.
- [25] ROSENFELD Y., SCHMIDT M., LÖWEN H. and TARAZONA P., *Phys. Rev. E*, **55** (1997) 4245.
- [26] BOUBLIK T., *J. Chem. Phys.*, **53** (1970) 471.
- [27] MANSOORI G. A., CARNAHAN N. F., STARLING K. E. and LELAND T. W. JR., *J. Chem. Phys.*, **54** (1971) 1523.
- [28] TARAZONA P., *Physica A*, **306** (2002) 243.
- [29] ROTH R., EVANS R., LANG. A. and KAHL. G., *J. Phys. Condens Matter*, **14** (2002) 12063.
- [30] YU Y.-X. and WU J., *J. Chem. Phys.*, **117** (2002) 10165.
- [31] EVANS R., *Adv. Phys.*, **28** (1979) 143.